The quantized Hall effect*

Klaus von Klitzing

Max-Planck-Institut für Festkörperforschung, D-7000 Stuttgart 80, West Germany

1. INTRODUCTION

Semiconductor research and the Nobel Prize in physics seem to be contradictory, since one may come to the conclusion that a complicated system like a semiconductor is not useful for very fundamental discoveries. Indeed, most of the experimental data in solid state physics are analyzed on the basis of simplified theories, and very often the properties of a semiconductor device are described by empirical formulas since the microscopic details are too complicated. Up to 1980 nobody expected that there exists an effect like the quantized Hall effect, which depends exclusively on fundamental constants and is not affected by irregularities in the semiconductor like impurities or interface effects.

The discovery of the quantized Hall effect (QHE) was the result of systematic measurements on silicon field effect transistors—the most important device in microelectronics. Such devices are important not only for applications but also for basic research. The pioneering work by Fowler, Fang, Howard, and Stiles (1966) has shown that new quantum phenomena become visible if the electrons of a conductor are confined within a typical length of 10 nm. Their discoveries opened the field of two-dimensional electron systems, which, since 1975, is the subject of a conference series.[1] It has been demonstrated that this field is important for the description of nearly all optical and electrical properties of microelectronic devices. A two-dimensional electron gas is absolutely necessary for the observation of the quantized Hall effect, and the realization and properties of such a system will be discussed in Sec. 2. In addition to the quantum phenomena connected with the confinement of electrons within a two-dimensional layer, another quantization—the Landau quantization of the electron motion in a strong magnetic field—is essential for the interpretation of the quantized Hall effect (Sec. 3). Some experimental results will be summarized in Sec. 4, and the application of the QHE in metrology is the subject of Sec. 5.

2. TWO-DIMENSIONAL ELECTRON GAS

The fundamental properties of the QHE are a consequence of the fact that the energy spectrum of the elec-

tronic system used for the experiments is a *discrete* energy spectrum. Normally, the energy E of mobile electrons in a semiconductor is quasicontinuous and can be compared with the kinetic energy of free electrons with wave vector k but with an effective mass m^*,

$$E = \frac{\hbar^2}{2m^*}(k_x^2 + k_y^2 + k_z^2) . \tag{1}$$

If the energy for the motion in one direction (usually the z direction) is fixed, one obtains a quasi-two-dimensional electron gas (2DEG), and a strong magnetic field perpendicular to the two-dimensional plane will lead—as discussed later—to a fully quantized energy spectrum, which is necessary for the observation of the QHE.

A two-dimensional electron gas can be realized at the surface of a semiconductor like silicon or gallium arsenide where the surface is usually in contact with a material which acts as an insulator (SiO_2 for silicon field effect transistors and, for example, $Al_xGa_{1-x}As$ for heterostructures). Typical cross sections of such devices are shown in Fig. 1. Electrons are confined close to the surface of the semiconductor by an electrostatic field F_z normal to the interface, originating from positive charges (see Fig. 1), which causes a drop in the electron potential towards the surface.

If the width of this potential well is small compared to the de Broglie wavelength of the electrons, the energy of the carriers is grouped in so-called electric subbands E_i corresponding to quantized levels for the motion in the z direction, the direction normal to the surface. In lowest approximation, the electronic subbands can be estimated by calculating the energy eigenvalues of an electron in a triangular potential with an infinite barrier at the surface ($z = 0$) and a constant electric field F_s for $z \geq 0$, which keeps the electrons close to the surface. The result of such calculations can be approximated by the equation
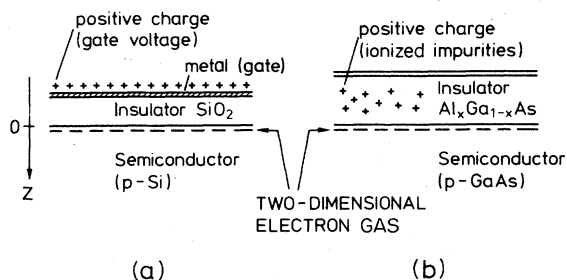

FIG. 1. Typical structures used for the realization of a two-dimensional electron gas (2DEG), which can be formed at the semiconductor surface if the electrons are fixed close to the surface by an external electric field: (a) Silicon MOSFET's; (b) GaAs-$Al_xGa_{1-x}As$ heterostructures.

---

*This lecture was delivered December 9, 1985, on the occasion of the presentation of the 1985 Nobel Prize in Physics.

[1]For a review, see the proceedings of the International Conference on Electronic Properties of Two-Dimensional Systems, published in Surf. Sci. **58** (1976), **73** (1978), **98** (1980), **113** (1982), and **142** (1984).

519
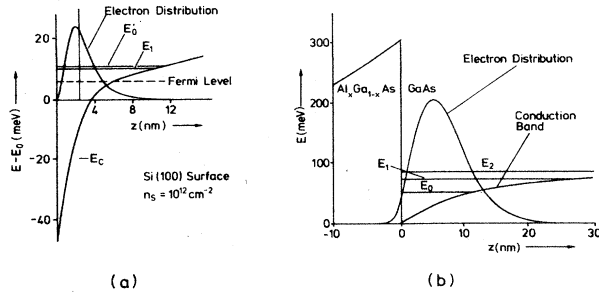
FIG. 2. Calculations of the electric subbands and the electron distribution within the surface channel of (a) a silicon MOSFET and (b) a GaAs-Al$_x$Ga$_{1-x}$As heterostructure (Stern and Howard, 1967; Ando, 1982).

$$E_j = \left[\frac{\hbar^2}{2m^*} \right]^{1/3} \cdot (\tfrac{3}{2}\pi e F_s)^{2/3} \cdot (j + \tfrac{3}{4})^{2/3} ,$$

$$j = 0, 1, 2, \ldots \quad (2)$$

In some materials, like silicon, different effective masses m^* and $m^{*\prime}$ may be present, which lead to different series E_j and E_j'.

Equation (2) must be incorrect if the energy levels E_j are occupied with electrons, since the electric field F_s will be screened by the electronic charge.

For a more quantitative calculation of the energies of the electric subbands, it is necessary to solve the Schrödinger equation for the actual potential V_z', which changes with the distribution of the electrons in the inversion layer. Typical results of such calculation for both silicon MOSFET's and GaAs heterostructures are shown in Fig. 2 (Stern and Howard, 1967; Ando, 1982). Usually, the electron concentration of the two-dimensional system is fixed for a heterostructure [Fig. 1(b)], but can be varied in a MOSFET by changing the gate voltage.

Experimentally, the separation between electric subbands, which is of the order of 10 meV, can be measured by analyzing the resonance absorption of electromagnetic waves with a polarization of the electric field perpendicular to the interface (Koch, 1975).

At low temperatures ($T < 4$ K) and small carrier densities for the 2DEG (Fermi energy E_F relative to the lowest electric subband E_0 small compared with the subband separation $E_1 - E_0$) only the lowest electric subband is occupied with electrons (electric quantum limit), which leads to a strictly two-dimensional electron gas with an energy spectrum

$$E = E_0 + \frac{\hbar^2 k_\parallel^2}{2m^*} , \quad (3)$$

where $k_\parallel$ is a wave vector within the two-dimensional plane.

For electrical measurements on a 2DEG, heavily doped n^+ contacts at the semiconductor surface are used as current contacts and potential probes. The shape of a typical sample used for QHE experiments (GaAs hetero-
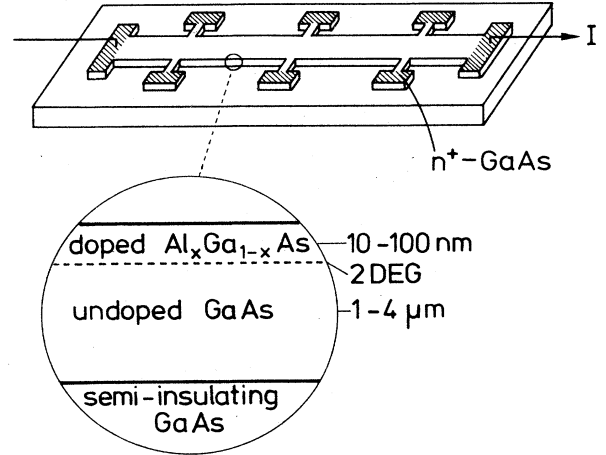

FIG. 3. Typical shape and cross section of a GaAs-Al$_x$Ga$_{1-x}$As heterostructure used for Hall-effect measurements.

structure) is shown in Fig. 3. The electrical current is flowing through the surface channel, since the fully depleted Al$_x$Ga$_{1-x}$As acts as an insulator (the same is true for the SiO$_2$ of a MOSFET) and the p-type semiconductor is electrically separated from the 2DEG by a p-n junction. It should be noted that the sample shown in Fig. 3 is basically identical with new devices which may be important for the next computer generation (Mimura, 1982). Measurements related to the quantized Hall effect which include an analysis and characterization of the 2DEG are therefore important for the development of devices, too.

3. QUANTUM TRANSPORT OF A 2DEG IN STRONG MAGNETIC FIELDS

A strong magnetic field B with a component B_z normal to the interface causes the electrons in the two-dimensional layer to move in cyclotron orbits parallel to the surface. As a consequence of the orbital quantization, the energy levels of the 2DEG can be written schematically in the form

$$E_n = E_0 + (n + \tfrac{1}{2})\hbar\omega_c + s \cdot g \cdot \mu_B \cdot B, \quad n = 0, 1, 2, \ldots , \quad (4)$$

with the cyclotron energy $\hbar\omega_c = \hbar e B / m^*$, the spin quantum number $s = \pm\tfrac{1}{2}$, the Landé factor g, and the Bohr magneton μ_B.

The wave function of a 2DEG in a strong magnetic field may be written in a form where the y coordinate y_0 of the center of the cyclotron orbit is a good quantum number (Laughlin, 1982),

$$\psi = e^{ikx} \Phi_n (y - y_0) , \quad (5)$$

where Φ_n is the solution of the harmonic-oscillator equation

$$\frac{1}{2m^*}[p_y^2+(eB)^2y^2]\Phi_n=(n+\tfrac{1}{2})\hbar\omega_c\Phi_n , \qquad (6)$$

and y_0 is related to k by

$$y_0=\hbar k/eB . \qquad (7)$$

The degeneracy factor for each Landau level is given by the number of center coordinates y_0 within the sample. For a given device with the dimensions $L_x \cdot L_y$, the center coordinates y_0 are separated by the amount

$$\Delta y_0=\frac{\hbar}{eB}\Delta k=\frac{\hbar}{eB}\frac{2\pi}{L_x}=\frac{h}{eBL_x} , \qquad (8)$$

so that the degeneracy factor $N_0=L_y/\Delta y_0$ is identical with $N_0=L_xL_yeB/h$, the number of flux quanta within the sample. The degeneracy factor per unit area is therefore

$$N=\frac{N_0}{L_xL_y}=\frac{eB}{h} . \qquad (9)$$

It should be noted that this degeneracy factor for each Landau level is independent of semiconductor parameters like effective mass.

In a more general way one can show (Kubo *et al.*, 1965) that the commutator for the center coordinates of the cyclotron orbit $[x_0,y_0]=i\hbar/eB$ is finite, which is equivalent to the result that each state occupies in real space the area $F_0=h/eB$ corresponding to the area of a flux quantum.

The classical expression for the Hall voltage U_H of a 2DEG with a surface carrier density n_s is

$$U_H=\frac{B}{n_s\cdot e}\cdot I , \qquad (10)$$

where I is the current through the sample. A calculation of the Hall resistance $R_H=U_H/I$ under the condition that i energy levels are fully occupied ($n_s=iN$) leads to the expression for the quantized Hall resistance

$$R_H=\frac{B}{iN\cdot e}=\frac{h}{ie^2}, \quad i=1,2,3,\ldots . \qquad (11)$$

A quantized Hall resistance is always expected if the carrier density n_s and the magnetic field B are adjusted in such a way that the filling factor i of the energy levels [Eq. (4)]

$$i=\frac{n_s}{eB/h} \qquad (12)$$

is an integer.

Under this condition the conductivity σ_{xx} (current flow in the direction of the electric field) becomes zero, since the electrons are moving like free particles exclusively perpendicular to the electric field and no diffusion (originating from scattering) in the direction of the electric field is possible. Within the self-consistent Born approximation (Ando, 1974) the discrete energy spectrum broadens as shown in Fig. 4(a). This theory predicts that the conductivity σ_{xx} is mainly proportional to the square
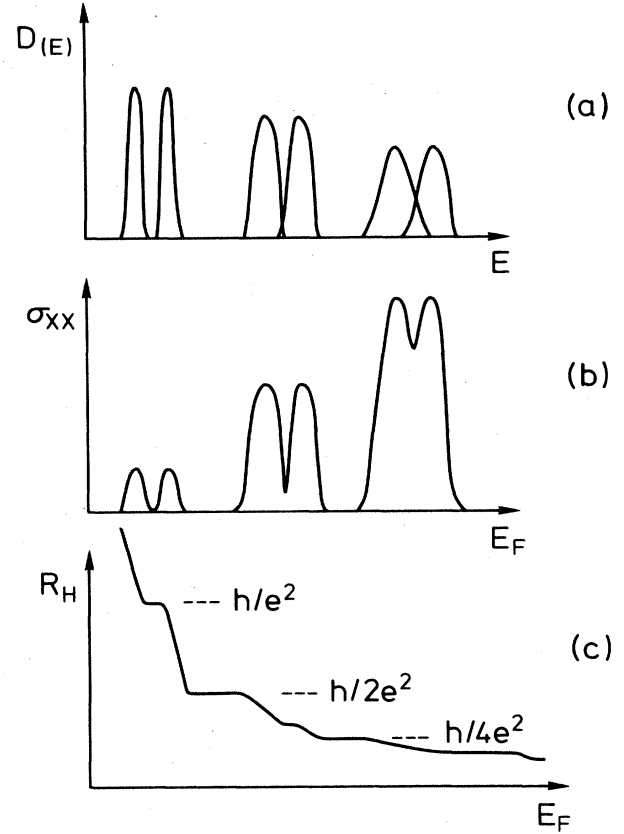

FIG. 4. Energy dependence of (a) the density of states, (b) conductivity σ_{xx}, and (c) Hall resistance R_H at a fixed magnetic field.

of the density of states at the Fermi energy E_F, which leads to a vanishing conductivity σ_{xx} in the quantum Hall regime and quantized plateaus in the Hall resistance R_H [Fig. 4(c)].

The simple one-electron picture for the Hall effect of an ideal two-dimensional system in a strong magnetic field leads already to the correct value for the quantized Hall resistance [Eq. (11)] at integer filling factors of the Landau levels. However, a microscopic interpretation of the QHE has to include the influences of the finite size of the sample, the finite temperature, the electron-electron interaction, impurities, and the finite current density (including the inhomogeneous current distribution within the sample) on the experimental result. Up to now, no corrections to the value h/ie^2 of the quantized Hall resistance are predicted if the conductivity σ_{xx} is zero. Experimentally, σ_{xx} is never exactly zero in the quantum Hall regime (see Sec. 4) but becomes unmeasurably small at high magnetic fields and low temperatures. A quantitative theory of the QHE has to include an analysis of the longitudinal conductivity σ_{xx} under real experimental conditions, and a large number of publications are discussing the dependence of the conductivity on the temperature, magnetic field, current density, sample size, etc.

The fact that the value of the quantized Hall resistance seems to be exactly correct for $\sigma_{xx}=0$ has led to the conclusion that a knowledge of microscopic details of the device is not necessary for a calculation of the quantized value. Consequently Laughlin (1984) tried to deduce the result in a more general way from gauge invariances. He considered the situation shown in Fig. 5. A ribbon of a two-dimensional system is bent into a loop and pierced everywhere by a magnetic field B normal to its surface. A voltage drop U_H is applied between the two edges of the ring. Under the condition of vanishing conductivity σ_{xx} (no energy dissipation), energy is conserved, and one can write Faraday's law of induction in a form that relates the current I in the loop to the adiabatic derivative of the total energy of the system E with respect to the magnetic flux φ threading the loop

$$I=\frac{\partial E}{\partial \varphi} .\tag{13}$$

If the flux is varied by a flux quantum $\varphi_0=h/e$, the wave function enclosing the flux must change by a phase factor 2π, corresponding to a transition of a state with wave vector k into its neighbor state $k+(2\pi)/(L_x)$, where L_x is the circumference of the ring. The total change in energy corresponds to a transport of states from one edge to the other with

$$\Delta E =i\cdot e\cdot U_H .\tag{14}$$

The integer i corresponds to the number of filled Landau levels if the free electron model is used, but can be, in principle, any positive or negative integer number.

From Eq. (13) the relation between the dissipationless Hall current and the Hall voltage can be deduced,

$$I =i\cdot e\cdot U_H/\varphi_0=i\frac{e^2}{h}\cdot U_H ,\tag{15}$$

which leads to the quantized Hall resistance $R_H =h/ie^2$.

In this picture the main reason for the Hall quantization is the flux quantization h/e and the quantization of charge into elementary charges e. In analogy, the frac-
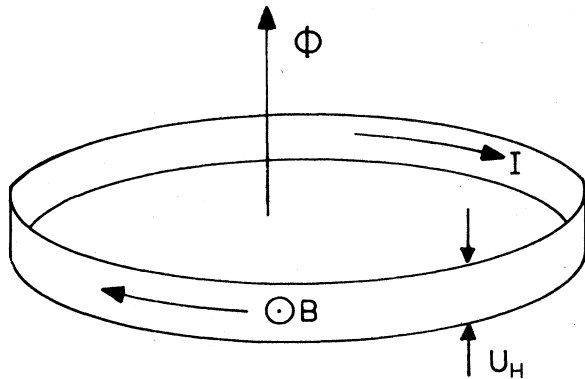

FIG. 5. Model of a two-dimensional metallic loop used for the derivation of the quantized Hall resistance.

tional quantum Hall effect, which will not be discussed in this paper, is interpreted on the basis of elementary excitations of quasiparticles with a charge $e^*=e/3,e/5,e/7$, etc.

The simple theory predicts that the ratio between the carrier density and the magnetic field has to be adjusted with very high precision in order to get exactly integer filling factors [Eq. (12)] and therefore quantized values for the Hall resistance. Fortunately, the Hall quantization is observed not only at special magnetic field values but in a wide magnetic field range, so that an accurate fixing of the magnetic field or the carrier density for high-precision measurements of the quantized resistance value is not necessary. Experimental data of such Hall plateaus are shown in the next section, and it is believed that localized states are responsible for the observed stabilization of the Hall resistance at certain quantized values.

After the discovery of the QHE a large number of theoretical papers were published discussing the influence of localized states on the Hall effect (Prange, 1981; Aoki and Ando, 1981; Chalker, 1983; Brenig, 1983); these calculations demonstrate that the Hall plateaus can be explained if localized states in the tails of the Landau levels are assumed. Theoretical investigations have shown that a mobility edge exists in the tails of Landau levels separating extended states from localized states (Ando, 1983; MacKinnon et al., 1984; Schweitzer et al., 1984; Aoki and Ando, 1985). The mobility edges are located close to the center of a Landau level for long-range potential fluctuations. Contrary to the conclusion reached by Abrahams et al. (1979), that all states of a two-dimensional system are localized, one has to assume that in a strong magnetic field at least one state of each Landau level is extended in order to observe a quantized Hall resistance. Some calculations indicate that the extended states are connected with edge states (Schweitzer et al., 1984).

In principle, an explanation of the Hall plateaus without including localized states in the tails of the Landau levels is possible if a reservoir of states is present outside the two-dimensional system (Baraff and Tsui, 1981; Toyoda et al., 1984). Such a reservoir for electrons, which should be in equilibrium with the 2DEG, fixes the Fermi energy within the energy gap between the Landau levels if the magnetic field or the number of electrons is changed. However, this mechanism seems to be more unlikely than localization in the tails of the Landau levels due to disorder. The following discussion assumes therefore a model with extended and localized states within one Landau level and a density of states as sketched in Fig. 6.

4. EXPERIMENTAL DATA

Magneto-quantum transport measurements on two-dimensional systems have been known and published for more than 20 years. The first data were obtained with sil-
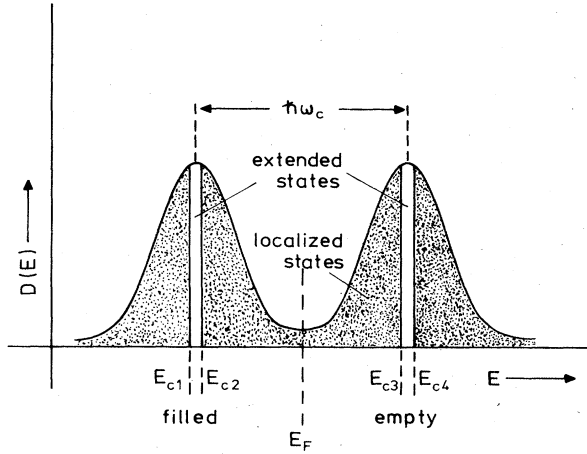
FIG. 6. Model for the broadened density of states of a 2DEG in a strong magnetic field. Mobility edges close to the center of the Landau levels separate extended states from localized states.

icon MOSFET's, and at the beginning mainly results for the conductivity σ_{xx} as a function of the carrier density (gate voltage) were analyzed. A typical curve is shown in Fig. 7. The conductivity oscillates as a function of the filling of the Landau levels and becomes zero at certain gate voltages V_g. In strong magnetic fields σ_{xx} vanishes, not only at a fixed value V_g, but in a range ΔV_g, and Kawaji was the first one who pointed out that some kind of immobile electrons must be introduced (Kawaji and Wakabayashi, 1976), since the conductivity σ_{xx} remains zero even if the carrier density is changed. However, no reliable theory was available for a discussion of localized electrons, whereas the peak value of σ_{xx} was well explained by calculations based on the self-consistent Born approximation and short-range scatterers which predict $\sigma_{xx} \sim (n + \frac{1}{2})$ independent of the magnetic field.

The theory for the Hall conductivity is much more complicated, and in the lowest approximation one expects that the Hall conductivity σ_{xy} deviates from the classical curve $\sigma_{xy}^0 = -n_s e /B$ (where n_s is the total number of elec-

trons in the two-dimensional system per unit area) by an amount $\Delta\sigma_{xy}$, which depends mainly on the third power of the density of states at the Fermi energy (Kawaji et al., 1975). However, no agreement between theory and experiment was obtained. Today, it is believed that $\Delta\sigma_{xy}$ is mainly influenced by localized states, which can explain the fact that not only a positive but also a negative sign for $\Delta\sigma_{xy}$ is observed. Up to 1980 all experimental Hall-effect data were analyzed on the basis of an incorrect model, so that the quantized Hall resistance, which is already visible in the data published in 1978 (Englert and von Klitzing, 1978), remained unexplained.

Whereas the conductivity σ_{xx} can be measured directly by using a Corbino disk geometry for the sample, the Hall conductivity is not directly accessible in an experiment but can be calculated from the longitudinal resistivity ρ_{xx} and the Hall resistivity ρ_{xy} measured on samples with Hall geometry (see Fig. 3):

$$\sigma_{xy} = -\frac{\rho_{xy}}{\rho_{xx}^2 + \rho_{xy}^2}, \quad \sigma_{xx} = \frac{\rho_{xx}}{\rho_{xx}^2 + \rho_{xy}^2} . \tag{16}$$

Figure 8 shows measurements for ρ_{xx} and ρ_{xy} of a silicon MOSFET as a function of the gate voltage at a fixed magnetic field. The corresponding σ_{xx} and σ_{xy} data are calculated on the basis of Eq. (16).

The classical curve $\sigma_{xy}^0 = -n_s e /B$ in Fig. 8 is drawn on the basis of the incorrect model, that the experimental data should lie always below the classical curve (=fixed sign for $\Delta\sigma_{xy}$) so that the plateau value σ_{xy} =const (observable in the gate voltage region where σ_{xx} becomes zero) should change with the width of the plateau. Wider plateaus should give smaller values for $|\sigma_{xy}|$. The main discovery in 1980 was (von Klitzing, Dorda, and Pepper, 1980) that the value of the Hall resistance in the plateau region is not influenced by the plateau width as shown in Fig. 9. Even the aspect ratio L/W (L =length, W =width of the sample), which normally influences the accuracy in Hall-effect measurements, becomes unimportant, as shown in Fig. 10. Usually, the measured Hall resistance R_H^{exp} is smaller than the theoretical value $R_H^{theor} = \rho_{xy}$ (von Klitzing, Ebert, et al., 1984; Rendell and Girvin, 1984)

$$R_H^{exp} = G \cdot R_H^{theor}, \quad G \leq 1 . \tag{17}$$

However, as shown in Fig. 11, the correction $1 - G$ becomes zero (independent of the aspect ratio) if $\sigma_{xx} \to 0$ or the Hall angle θ approaches $90°$ ($\tan\theta = \sigma_{xy}/\sigma_{xx}$). This means that any shape of the sample can be used in QHE experiments as long as the Hall angle is $90°$ (or $\sigma_{xx} = 0$). However, outside the plateau region ($\sigma_{xx} \sim \rho_{xx} \neq 0$) the measured Hall resistance $R_H^{exp} = U_H /I$ is indeed always smaller than the theoretical ρ_{xy} value (von Klitzing,
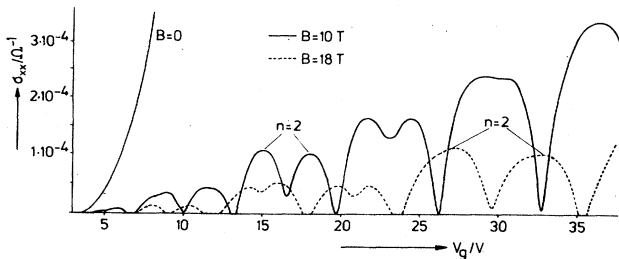

FIG. 7. Conductivity σ_{xx} of a silicon MOSFET at different magnetic fields B as a function of the gate voltage V_g.
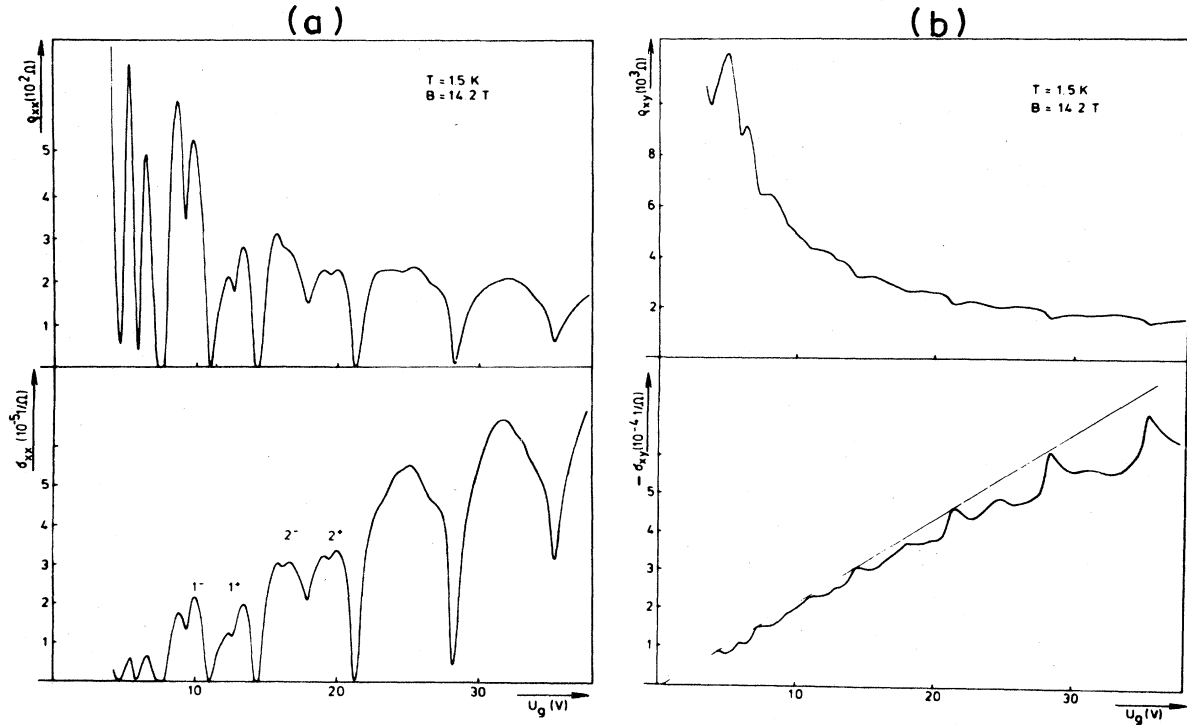
(a)

(b)

FIG. 8. Measured ρ_{xx} and ρ_{xy} data of a silicon MOSFET as a function of the gate voltage at $B = 14.2$ T together with the calculated σ_{xx} and σ_{xy} curves.

1981). This leads to the experimental result that an additional minimum in R_H^{exp} becomes visible outside the plateau region, as shown in Fig. 9, which disappears if the correction due to the finite length of the sample is included (see Fig. 12). The first high-precision measurements in 1980 of the plateau value in R_H (V_g) showed already that these resistance values are quantized in integer parts of $h/e^2 = 25\,812$, 8 Ω within the experimental uncertainty of 3 ppm.
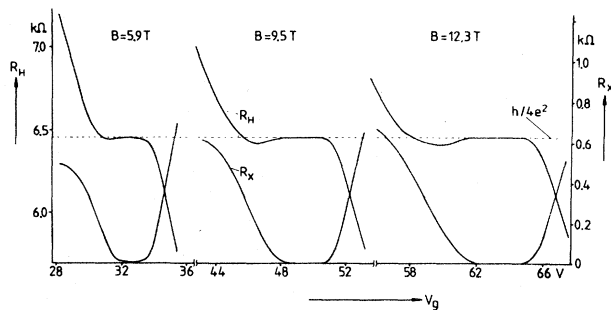
FIG. 9. Measurements of the Hall resistance R_H and the resistivity R_x as a function of the gate voltage at different magnetic field values. The plateau values $R_H = h/4e^2$ are independent of the width of the plateaus.
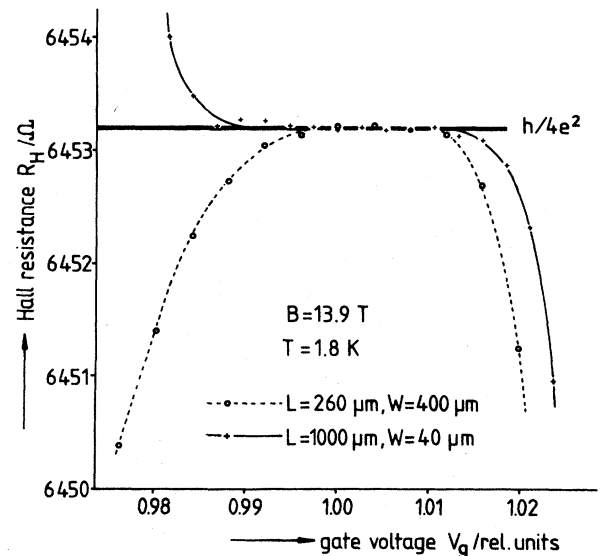
FIG. 10. Hall resistance R_H for two different samples with different aspect ratios L/W as a function of the gate voltage ($B = 13.9$ T).
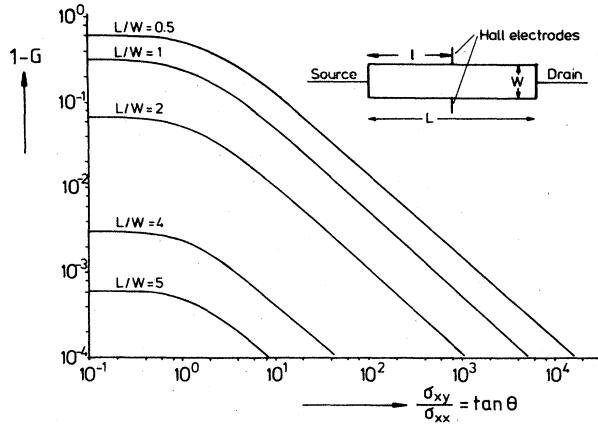
FIG. 11. Calculations of the correction term G in Hall-resistance measurements due to the finite length-to-width ratio L/W of the device $(l/L = 0.5)$.

FIG. 13. Measured curves for the Hall resistance R_H and the longitudinal resistance R_x of a GaAs-Al$_x$Ga$_{1-x}$As heterostructure as a function of the gate voltage at different magnetic fields.

The Hall plateaus are much more pronounced in measurements on GaAs-Al$_x$Ga$_{1-x}$As heterostructures, since the small effective mass m^* of the electrons in GaAs $[m^*(\text{Si})/m^*(\text{GaAs}) > 3]$ leads to a relatively large energy splitting between Landau levels [Eq. (4)], and the high quality of the GaAs-Al$_x$Ga$_{1-x}$As interface (nearly no surface roughness) leads to a high mobility μ of the electrons, so that the condition $\mu B > 1$ for Landau quantizations is fulfilled already at relatively low magnetic fields. Figure 13 shows that well-developed Hall plateaus are visible for this material already at a magnetic field
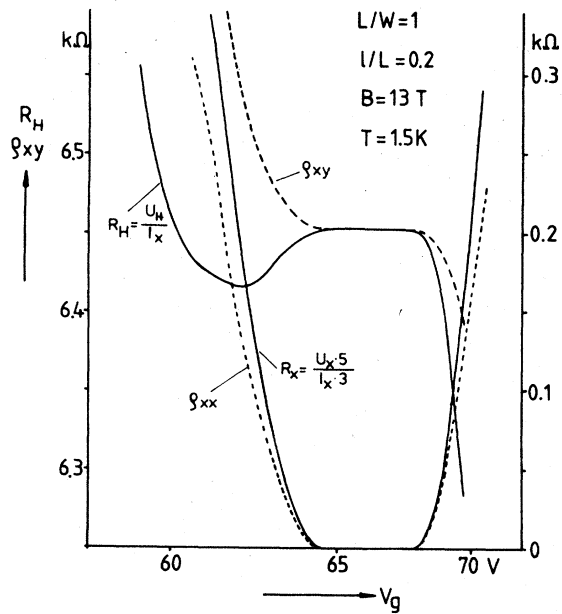
strength of 4 tesla. Since a finite carrier density is usually present in heterostructures, even at a gate voltage $V_g = 0$ V, most of the published transport data are based on measurements without applied gate voltage as a function of the magnetic field. A typical result is shown in Fig. 14. The Hall resistance $R_H = \rho_{xy}$ shows steplike increases with plateaus in the magnetic field region where the long-

FIG. 12. Comparison between the measured quantities R_H and R_x and the corresponding resistivity components ρ_{xy} and ρ_{xx}, respectively.
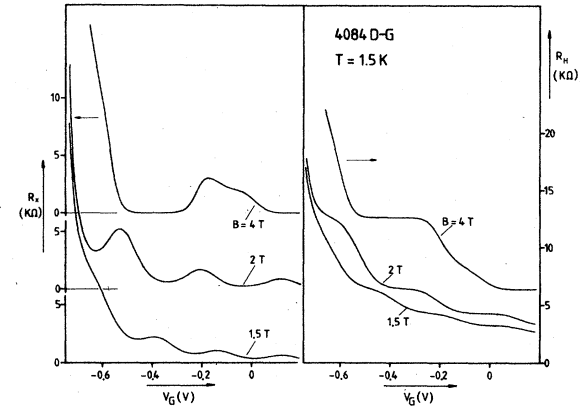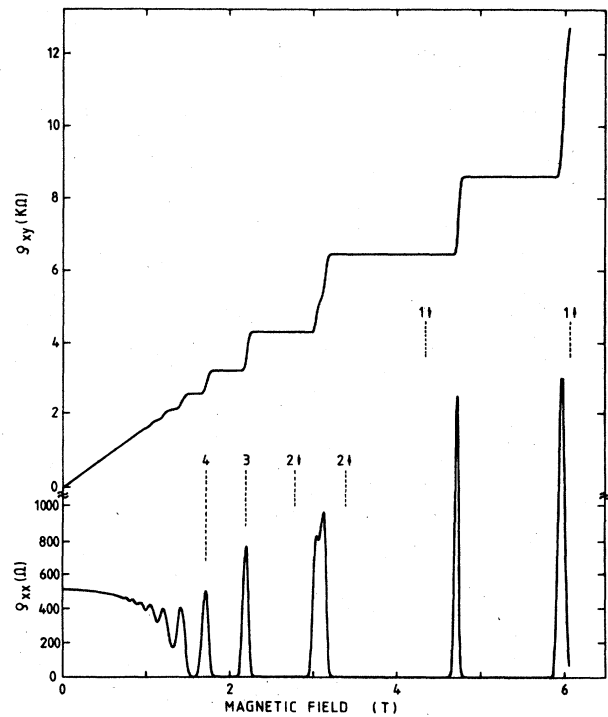

FIG. 14. Experimental curves for the Hall resistance $R_H = \rho_{xy}$ and the resistivity $\rho_{xx} \sim R_x$ of a heterostructure as a function of the magnetic field at a fixed carrier density corresponding to a gate voltage $V_g = 0$ V. The temperature is about 8 mK.
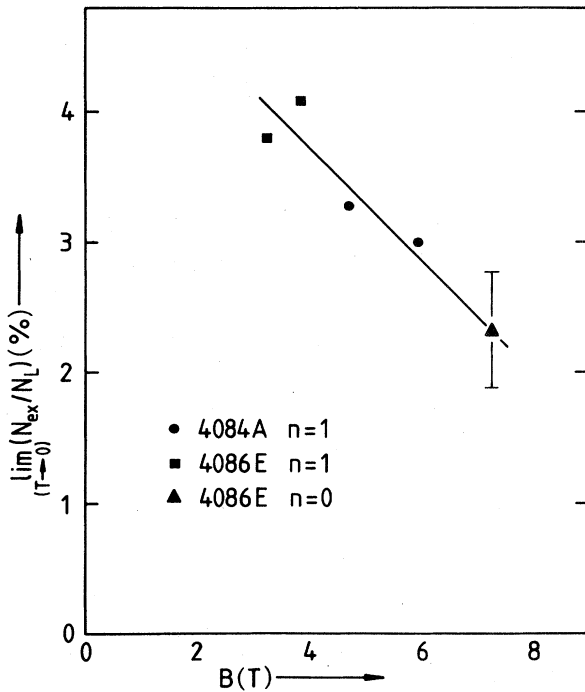
FIG. 15. Fraction of extended states relative to the number of states of one Landau level as a function of the magnetic field.
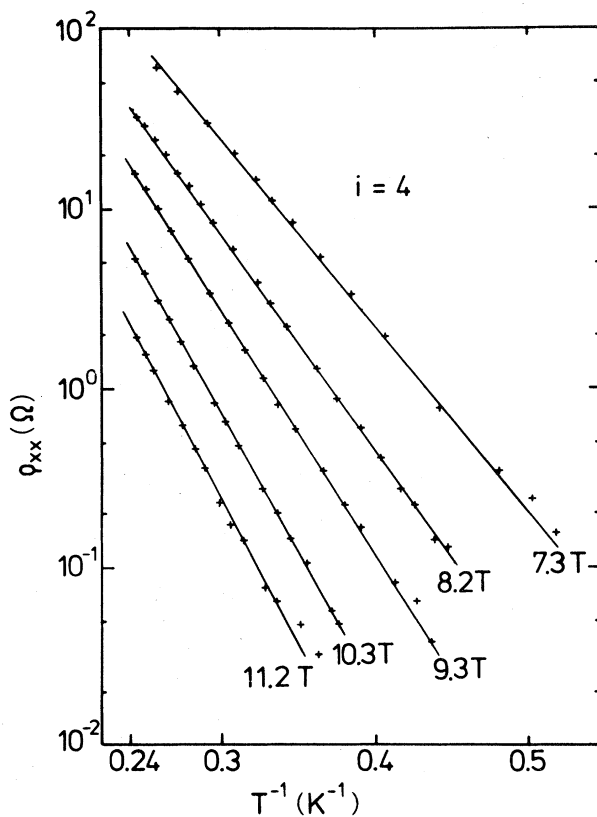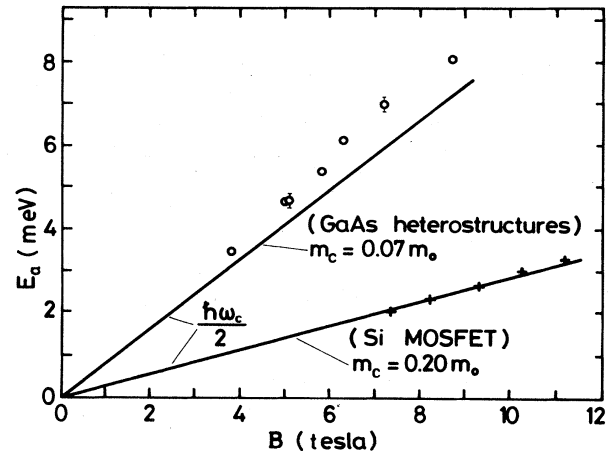
FIG. 17. Measured activation energies at filling factors $i = 2$ (GaAs heterostructure) or $i = 4$ (Si MOSFET) as a function of the magnetic field. The data are compared with the energy $0.5\hbar\omega_c$.

itudinal resistance ρ_{xx} vanishes. The width of the ρ_{xx} peaks in the limit of zero temperature can be used for a determination of the number of extended states, and the analysis (Ebert *et al.*, 1982) shows that only a few percent of the states of a Landau level are not localized. The fraction of extended states within one Landau level decreases with increasing magnetic field (Fig. 15), but the number of extended states within each level remains approximately constant, since the degeneracy of each Landau level increases proportional to the magnetic field.

FIG. 16. Thermally activated resistivity ρ_{xx} at a filling factor $i = 4$ for a silicon MOSFET at different magnetic field values.
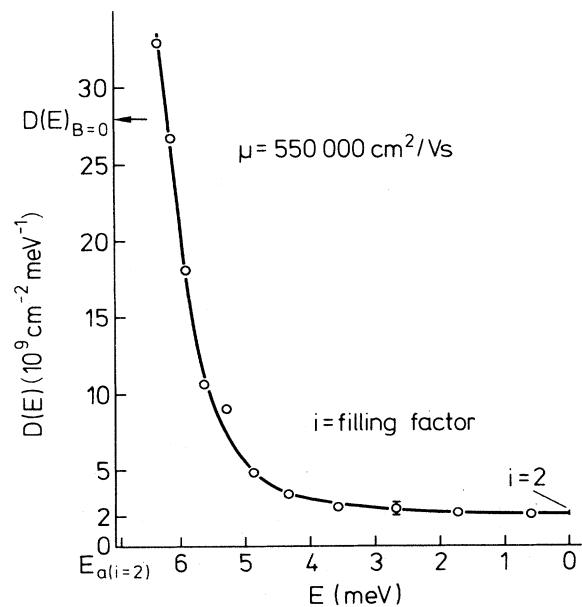
FIG. 18. Measured density of states (deduced from an analysis of the activated resistivity) as a function of the energy relative to the center between two Landau levels. (GaAs heterostructure.)

At finite temperatures ρ_{xx} is never exactly zero, and the same is true for the slope of the ρ_{xy} curve in the plateau region. But in reality, the slope $d\rho_{xy}/dB$ at $T < 2$ K and magnetic fields above 8 tesla is so small that the ρ_{xy} value stays constant within the experimental uncertainty of 6×10^{-8} even if the magnetic field is changed by 5%. Simultaneously the resistivity ρ_{xx} is usually smaller than 1 mΩ. However, at higher temperatures or lower magnetic fields a finite resistivity ρ_{xx} and a finite slope $d\rho_{xy}/dn_s$ (or $d\rho_{xy}/dB$) can be measured. The data are well described within the model of extended states at the energy position of the undisturbed Landau level E_n and a finite density of localized states between the Landau levels (mobility gap). As in amorphous systems, the temperature dependence of the conductivity σ_{xx} (or resistivity ρ_{xx}) is thermally activated, with an activation energy E_a corresponding to the energy difference between the Fermi energy E_F and the mobility edge. The largest activation energy with a value $E_a = \frac{1}{2}\hbar\omega_c$ (if the spin splitting is negligibly small and the mobility edge is located at the center E_n of a Landau level) is expected if the Fermi energy is located exactly at the midpoint between two Landau levels.

Experimentally, an activated resistivity

$$\rho_{xx} \sim \exp[-(E_a/kT)] \tag{18}$$

is observed in a wide temperature range for different two-dimensional systems (deviations from this behavior, which appear mainly at temperatures below 1 K, will be discussed separately), and a result is shown in Fig. 16. The activation energies (deduced from these data) are plotted in Fig. 17 for both silicon MOSFET's and GaAs-Al$_x$Ga$_{1-x}$As heterostructures as a function of the magnetic field; the data agree fairly well with the expected curve $E_a = \frac{1}{2}\hbar\omega_c$. Up to now, it is not clear whether the small systematic shift of the measured activation energies to higher values originates from a temperature-dependent prefactor in Eq. (18) or is a result of the enhancement of the energy gap due to many-body effects.

The assumption that the mobility edge is located close to the center of a Landau level E_n is supported by the fact that for the samples used in the experiments only a few percent of the states of a Landau level are extended (Ebert et al., 1982). From a systematic analysis of the activation energy as a function of the filling factor of a Landau level it is possible to determine the density of states $D(E)$ (Stahl et al., 1985). The surprising result is that the density of states (DOS) is finite and approximately constant within 60% of the mobility gap, as shown in Fig. 18. This background DOS depends on the electron mobility as summarized in Fig. 19.

An accurate determination of the DOS close to the center of the Landau level is not possible by this method, since the Fermi energy becomes temperature dependent if the DOS changes drastically within the energy range of 3 kT. However, from an analysis of the capacitance C as a function of the Fermi energy, the peak value of the DOS and its shape close to E_n can be deduced (Smith et al.,
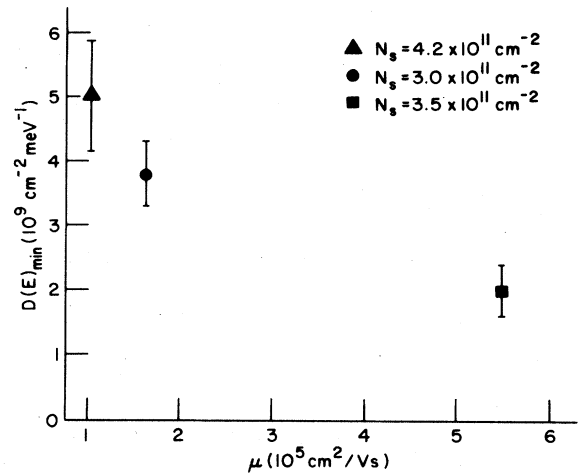

FIG. 19. Background density of states as a function of the mobility of the device.

1985; Mosser et al., 1986).

This analysis is based on the equation

$$\frac{1}{C} = \frac{1}{e^2 \cdot D(E_F)} + \text{const} . \tag{19}$$

The combination of the different methods for the determination of the DOS leads to a result like that shown in Fig. 20. Similar results are obtained from other experiments (Gornik et al., 1985; Eisenstein et al., 1986), but no theoretical explanation is available.
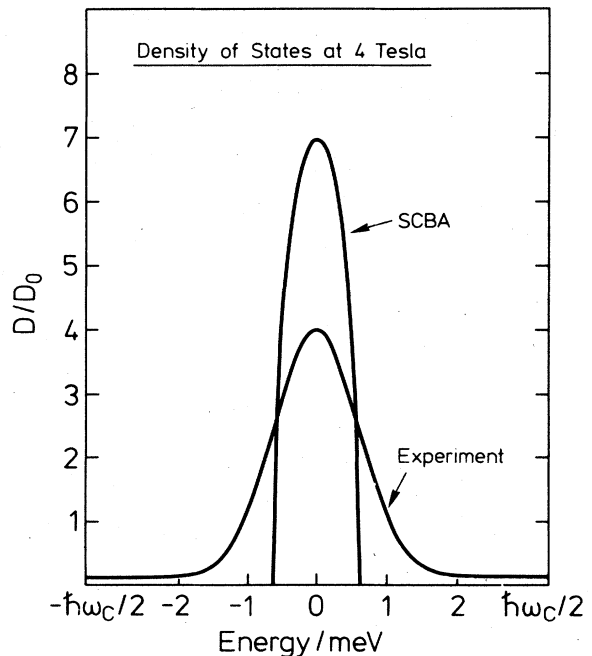

FIG. 20. Experimentally deduced density of states of a GaAs heterostructure at $B = 4$ T compared with the calculated result based on the self-consistent Born approximation (SCBA).
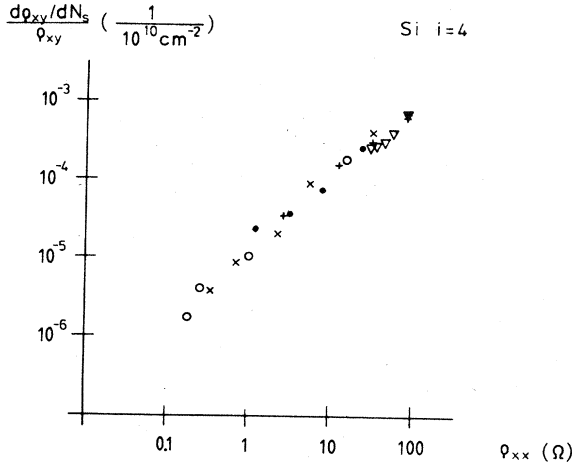
FIG. 21. Relation between the slope of the Hall plateaus $d\rho_{xy}/dn_s$ and the corresponding ρ_{xx} value at integer filling factors.

If one assumes that only the occupation of extended states influences the Hall effect, then the slope $d\rho_{xy}/dn_s$ in the plateau region should be dominated by the same activation energy as found for $\rho_{xx}(T)$. Experimentally (Tausendfreund and von Klitzing, 1984), a one-to-one relation between the minimal resistivity ρ_{xx}^{min} at integer filling factors and the slope of the Hall plateau has been found (Fig. 21), so that the flatness of the plateau increases with decreasing resistivity, which means lower temperature or higher magnetic fields.
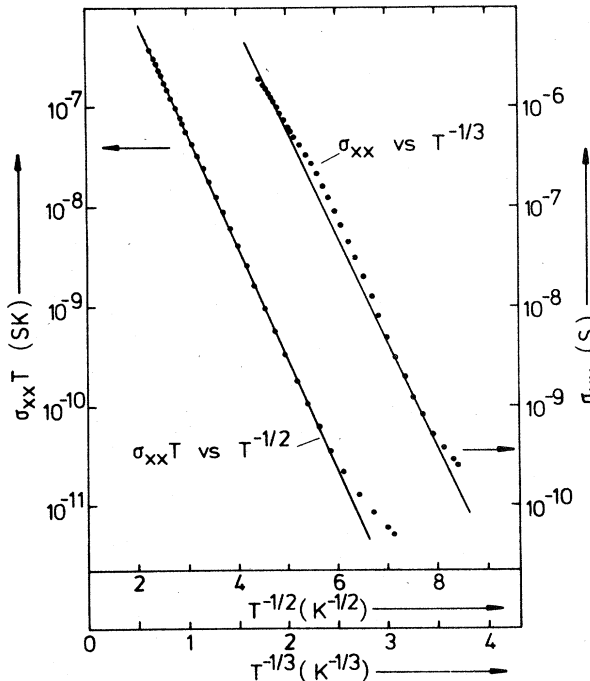

FIG. 22. Analysis of the temperature-dependent conductivity of a GaAs heterostructure (filling factor $i = 3$) at $T < 0.2$ K.
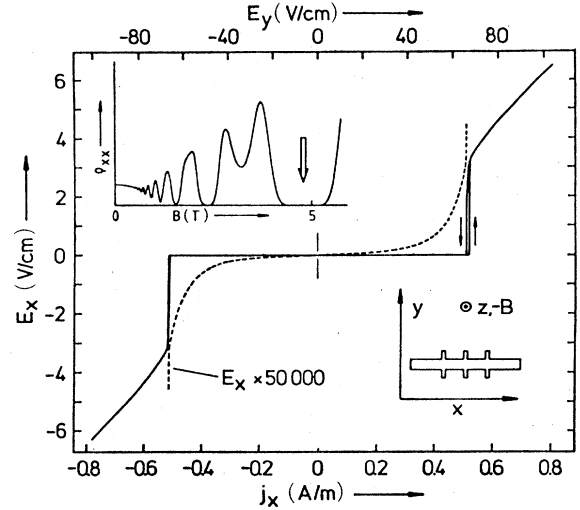

FIG. 23. Current-voltage characteristic of a GaAs-$Al_xGa_{1-x}As$ heterostructure at a filling factor $i = 2$ ($T = 1.4$ K). The device geometry and the $\rho_{xx}(B)$ curve are shown in the insets.

The temperature dependence of the resistivity deviates from an activated behavior at low temperatures, typically at $T < 1$ K. Such deviations are found in measurements on disordered systems, too, and are interpreted as variable-range hopping. For a two-dimensional system with exponentially localized states, a behavior

$$\rho_{xx} \sim \exp[-(T_0/T)^{1/3}] \tag{20}$$

is expected. For a Gaussian localization the following dependence is predicted (Pepper, 1978; Ono, 1982):

$$\rho_{xx} \sim \frac{1}{T} \exp[-(T_0/T)^{1/2}] . \tag{21}$$

The analysis of the experimental data demonstrates (Fig. 22) that the measurements are best described on the basis of Eq. (21). The same behavior has been found in measurements on another two-dimensional system, on InP-InGaAs heterostructures (Guldner et al., 1984).

The contribution of the variable-range hopping process to the Hall effect is negligibly small (Wysokinski and Brenig, 1983), so that experimentally the temperature dependence of $d\rho_{xy}/dn_s$ remains thermally activated even if the resistivity ρ_{xx} is dominated by variable-range hopping.

The QHE breaks down if the Hall field becomes larger than about $E_H = 60$ V/cm at magnetic fields of 5 tesla. This corresponds to a classical drift velocity $v_D = E_H/B \approx 1200$ m/s. At the critical Hall field E_H (or current density j) the resistivity increases abruptly by orders of magnitude and the Hall plateau disappears. This phenomenon has been observed by different authors for different materials (Ebert et al., 1983; Cage et al., 1983; Kuchar, Bauer et al., 1984; Kuchar, Meisels et al., 1984; Sakaki et al., 1984; von Klitzing, Ebert et al., 1984; Störmer et al., 1984; Pudalov and Semenchinsky, 1984). A typical result is shown in Fig. 23. At a current density
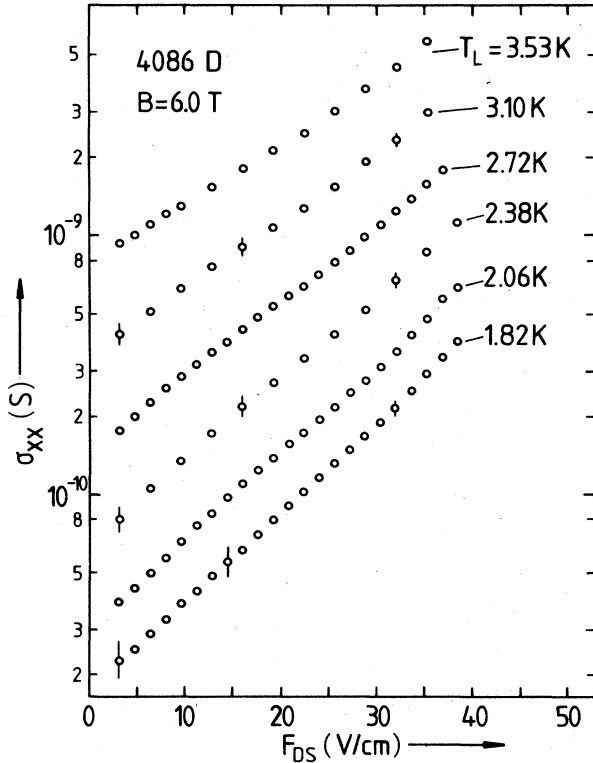
FIG. 24. Nonohmic conductivity σ_{xx} of a GaAs heterostructure at different temperatures T_L (filling factor $i = 2$). An instability is observed at source-drain fields larger than 40 V/cm.

of $j_c = 0.5$ A/m, the resistivity ρ_{xx} at the center of the plateau (filling factor $i = 2$) increases drastically. This instability, which develops within a time scale of less than 100 ns, seems to originate from a runaway in the electron temperature, but other mechanisms like electric-field-dependent delocalization, Zener tunneling, or emission of acoustic phonons, if the drift velocity exceeds the sound velocity, can be used for an explanation (Trugman, 1983; Streda and von Klitzing, 1984; Heinomen et al., 1984).

Figure 23 shows that ρ_{xx} increases already at current densities well below the critical value j_c, which may be explained by a broadening of the extended state region and therefore a reduction in the mobility gap ΔE. If the resistivity ρ_{xx} is thermally activated and the mobility gap changes linearly with the Hall field (which is proportional to the current density j), then a variation $\ln \rho_{xx} \sim j$ is expected. Such a dependence is seen in Fig. 24, but a quantitative analysis is difficult since the current distribution within the sample is usually inhomogeneous and the Hall field, calculated from the Hall voltage and the width of the sample, represents only a mean value. Even for an ideal two-dimensional system an inhomogeneous Hall potential distribution across the width of the sample is expected (MacDonald et al., 1983; Reiss, 1984; Heinonen and Taylor, 1985) with an enhancement of the current density close to the boundaries of the sample.
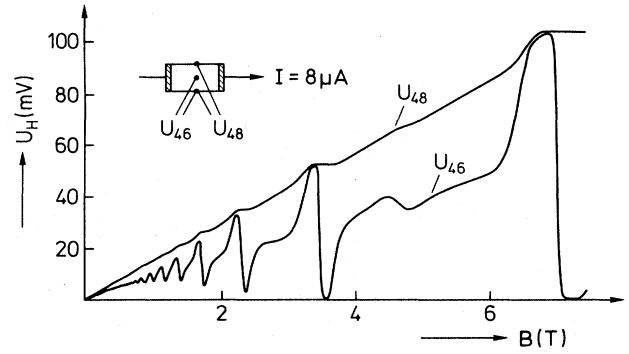

FIG. 25. Measured Hall potential distribution of a GaAs heterostructure as a function of the magnetic field.

The experimental situation is still more complicated, as shown in Fig. 25. The potential distribution depends strongly on the magnetic field. Within the plateau region the current path moves with increasing magnetic field across the width of the sample from one edge to the other. A gradient in the carrier density within the two-dimensional system seems to be the most plausible explanation, but in addition an inhomogeneity produced by the current itself may play a role. Up to now, not enough microscopic details about the two-dimensional system are known, so that at present a microscopic theory that describes the QHE under real experimental conditions is not available. However, all experiments and theories indicate that in the limit of vanishing resistivity ρ_{xx} the value of the quantized Hall resistance depends exclusively on fundamental constants. This leads to a direct application of the QHE in metrology.

5. APPLICATION OF THE QUANTUM HALL EFFECT IN METROLOGY

The applications of the quantum Hall effect are very similar to the applications of the Josephson effect, which can be used for the determination of the fundamental constant h/e or for the realization of a voltage standard. In analogy, the QHE can be used for a determination of h/e^2 or as a resistance standard (von Klitzing and Ebert, 1985).

Since the inverse fine-structure constant α^{-1} is more or less identical with h/e^2 (the proportional constant is a fixed number that includes the velocity of light), high-precision measurements of the quantized Hall resistance are important for all areas in physics that are connected with the fine-structure constant.

Experimentally, the precision measurement of α is reduced to the problem of measuring an electrical resistance with high accuracy, and the different methods and results are summarized in the Proceedings of the 1984 Conference on Precision Electromagnetic Measurements
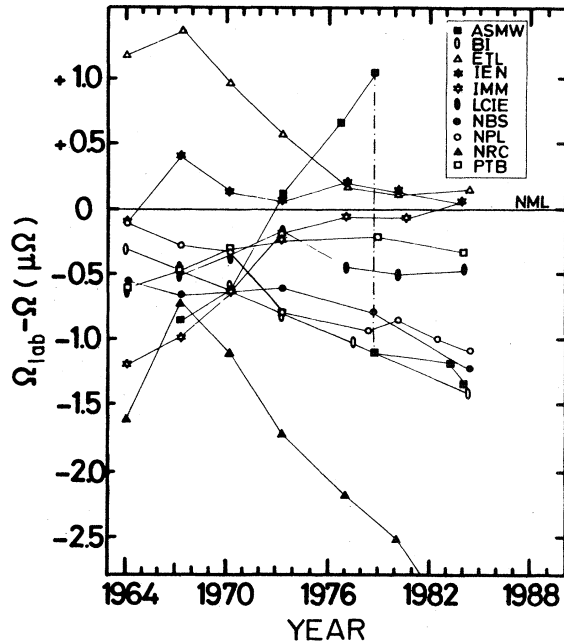
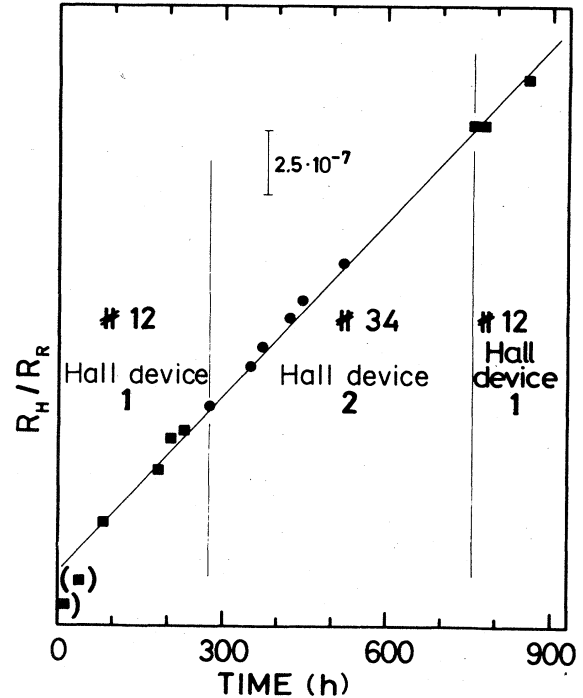FIG. 26. Time dependence of the 1-Ω standard resistors maintained at the different national laboratories.

FIG. 27. Ratio R_H/R_R between the quantized Hall resistance R_H and a wire resistor R_R as a function of time. The result is time dependent but independent of the Hall device used in the experiment.

(CPEM, 1984).[2] The mean value of measurements at laboratories in three different countries is

$$\alpha^{-1} = 137.035\,988 \pm 0.000\,02 \ .$$

The internationally recommended value (Cohen and Taylor, 1973) is

$$\alpha^{-1} = 137.036\,04 \pm 0.000\,11 \ ,$$

and the preliminary value for the fine-structure constant based on a new least-squares adjustment of fundamental constants (1985) is

$$\alpha^{-1} = 137.035\,991 \pm 0.000\,008 \ .$$

Different groups have demonstrated that the experimental result is within an experimental uncertainty of less than 3.7×10^{-8} independent of the material (Si, GaAs, $In_{0.53}Ga_{0.47}As$) and of the growing technique of the devices (MBE or MOCVD) (Delahaye et al., 1986). The main problem in high-precision measurements of α is—at present—the calibration and stability of the reference resistor. Figure 26 shows the drift of the maintained 1-Ω resistor at different national laboratories. The very first application of the QHE is the determination of the drift coefficient of the standard resistors, since the quantized Hall resistance is more stable and more reproducible than

any wire resistor. A nice demonstration of such an application is shown in Fig. 27. In this experiment the quantized Hall resistance R_H has been measured at the Physikalisch Technische Bundesanstalt relative to a reference resistor R_R as a function of time. The ratio R_H/R_R changes approximately linearly with time, but the result is independent of the QHE sample. This demonstrates that the reference resistor changes its value with time. The one standard deviation of the experimental data from the mean value is only 2.4×10^{-8}, so that the QHE can already be used today as a relative standard to maintain a laboratory unit of resistance based on wire-wound resistors. There exists an agreement that the QHE should be used as an absolute resistance standard if three independent laboratories measure the same value for the quantized Hall resistance (in SI units) with an uncertainty of less than 2×10^{-7}. It is expected that these measurements will be finished by the end of 1986.

ACKNOWLEDGMENTS

---

[2]High-precision measurements of the quantized Hall resistance are summarized in IEEE Trans. Instrum. Meas. **IM-34**, 301–327.

work at the time of the discovery of the QHE in 1980. Primarily, I would like to thank G. Dorda (Siemens Forschungslaboratorien) and M. Pepper (Cavendish Laboratory, Cambridge) for providing me with high-quality MOS devices. The continuous support of my research work by G. Landwehr and the fruitful discussions with my co-worker, T. Englert, were essential for the discovery of the quantum Hall effect and are gratefully acknowledged.

REFERENCES

Abrahams, E., P. W. Anderson, D. C. Licciardello, and T. V. Ramakrishnan, 1979, Phys. Rev. Lett. 42, 673.

Ando, T., 1974, J. Phys. Soc. Jpn. 37, 1233.

Ando, T., 1982, J. Phys. Soc. Jpn. 51, 3893.

Ando, T., 1983, J. Phys. Soc. Jpn. 52, 1740.

Aoki, H., and T. Ando, 1981, Solid State Commun. 38, 1079.

Aoki, H., and T. Ando, 1985, Phys. Rev. Lett. 54, 831.

Baraff, G. A., and D. C. Tsui, 1981, Phys. Rev. B 24, 2274.

Brenig, W., 1983, Z. Phys. B 50, 305.

Cage, M. E., R. F. Dziuba, B. F. Field, E. R. Williams, S. M. Girvin, A. C. Gossard, D. C. Tsui, and R. J. Wagner, 1983, Phys. Rev. Lett. 51, 1374.

Chalker, J. T., 1983, J. Phys. C 16, 4297.

Cohen, E. R., and B. N. Taylor, 1973, J. Phys. Chem. Ref. Data 2, 663.

CPEM, 1984, Conference on Precision Electromagnetic Measurements, summarized in IEEE Trans. Instrum. Meas. 34, 301.

Delahaye, F., D. Dominguez, F. Alexandre, J. P. Andre, J. P. Hirtz, and M. Razeghi, 1986, Metrologia 22, 103.

Ebert, G., K. von Klitzing, K. Ploog, and G. Weimann, 1983, J. Phys. C 16, 5441.

Ebert, G., K. von Klitzing, C. Probst, and K. Ploog, 1982, Solid State Commun. 44, 95.

Eisenstein, J. P., H. L. Störmer, V. Narayanamurti, A. Y. Cho, and A. C. Gossard, 1986, in *Proceedings of the 6th International Conference on Electronic Properties of Two-Dimensional Systems* (Yamada Conference XIII) [Surf. Sci. (in press)], p. 292.

Englert, T., and K. von Klitzing, 1978, Surf. Sci. 73, 70.

Fowler, A. B., F. F. Fang, W. E. Howard, and P. J. Stiles, 1966, Phys. Rev. Lett. 16, 901.

Gornick, E., R. Lassnig, G. Strasser, H. L. Störmer, A. C. Gossard, and W. Wiegmann, 1985, Phys. Rev. Lett. 54, 1820.

Guldner, Y., J. P. Hirtz, A. Briggs, J. P. Vieren, M. Voos, and M. Razeghi, 1984, Surf. Sci. 142, 179.

Heinonen, O., and P. L. Taylor, 1985, Phys. Rev. B 32, 633.

Heinonen, O., P. L. Taylor, and S. M. Girvin, 1984, Phys. Rev. B 30, 3016.

Kawaji, S., T. Igarashi, and J. Wakabayashi, 1975, Prog. Theor. Phys. 57, 176.

Kawaji, S., and J. Wakabayashi, 1976, Surf. Sci. 58, 238.

Koch, J. F., 1975, Festkörperprobleme 15, 79.

Kubo, R., S. J. Miyake, and N. Hashitsume, 1965, in *Solid State Physics*, edited by F. Seitz and D. Turnbull (Academic, New York), Vol. 17, p. 269.

Kuchar, F., G. Bauer, G. Weimann, and H. Burkhard, 1984,

Surf. Sci. 142, 196.

Kuchar, F., R. Meisels, G. Weimann, and H. Burkhard, 1984, in *Proceedings of the 17th International Conference on the Physics of Semiconductors, 1984*, edited by James D. Chadi and Walter A. Harrison (Springer, Berlin/New York), p. 275.

Laughlin, R. B., 1982, Surf. Sci. 113, 22.

Laughlin, R. B., 1984, in *Two-Dimensional Systems, Heterostructures, and Superlattices* . . . , Springer Series in Solid State Sciences No. 53, edited by G. Bauer, F. Kuchar, and H. Heinrich (Springer, Berlin/New York), p. 272.

MacDonald, A. H., T. M. Rice, and W. F. Brinkman, 1983, Phys. Rev. B 28, 3648.

MacKinnon, A., L. Schweitzer, and B. Kramer, 1984, Surf. Sci. 142, 189.

Mimura, T., 1982, Surf. Sci. 113, 454.

Mosser, V., D. Weiss, K. von Klitzing, K. Ploog, and G. Weimann, 1986, Solid State Commun. 58, 5.

Ono, Y., 1982, J. Phys. Soc. Jpn. 51, 237.

Pepper, M., 1978, Philos. Mag. 37, 83.

Prange, R. E., 1981, Phys. Rev. B 23, 4802.

Pudalov, V. M., and S. G. Semenchinsky, 1984, Solid State Commun. 51, 19.

Reiss, J., 1984, J. Phys. C 17, L849.

Rendell, R. W., and S. M. Girvin, 1984, in *Precision Measurement and Fundamental Constants*, edited by B. N. Taylor and W. D. Phillips, National Bureau of Standards (U.S.) Special Publication No. 617, p. 557.

Sakaki, H., K. Hirakawa, J. Yoshino, S. P. Svensson, Y. Sekiguchi, T. Hotta, and S. Nishii, 1984, Surf. Sci. 142, 306.

Schweitzer, L., B. Kramer, and A. MacKinnon, 1984, J. Phys. C 17, 4111.

Smith, T. P., B. B. Goldberg, P. J. Stiles, and M. Heiblum, 1985, Phys. Rev. B 32, 2696.

Stahl, E., D. Weiss, G. Weimann, K. von Klitzing, and K. Ploog, 1985, J. Phys. C 18, L783.

Stern, F., and W. E. Howard, 1967, Phys. Rev. 163, 816.

Störmer, H. L., A. M. Chang, D. C. Tsui, and J. C. M. Hwang, 1984, in *Proceedings of the 17th International Conference on the Physics of Semiconductors, 1984*, edited by James D. Chadi and Walter A. Harrison (Springer, Berlin/New York), p. 267.

Streda, P., and K. von Klitzing, 1984, J. Phys. C 17, L483.

Tausendfreund, B., and K. von Klitzing, 1984, Surf. Sci. 142, 220.

Toyoda, T., V. Gudmundsson, and Y. Takahashi, 1984, Phys. Lett. A 102, 130.

Trugman, S. A., 1983, Phys. Rev. B 27, 7539.

von Klitzing, K., 1981, Festkörperprobleme 21, 1.

von Klitzing, K., G. Dorda, and M. Pepper, 1980, Phys. Rev. Lett. 45, 494.

von Klitzing, K., and G. Ebert, 1985, Metrologia 21, 11.

von Klitzing, K., G. Ebert, N. Kleinmichel, H. Obloh, D. Dorda, and G. Weimann, 1984, in *Proceedings of the 17th International Conference on the Physics of Semiconductors, 1984*, edited by James D. Chadi and Walter A. Harrison (Springer, Berlin/New York), p. 271.

von Klitzing, K., H. Obloh, G. Ebert, K. Knecht, and K. Ploog, 1984, in *Precision Measurement and Fundamental Constants*, edited by B. N. Taylor and W. D. Phillips, National Bureau of Standards (U.S.) Special Publication No. 617, p. 526.

Wysokinski, K. I., and W. Brenig, 1983, Z. Phys. B 54, 11.